SUPPLEMENTARY ONLINE DATA

Substrate inhibition of the betaine aldehyde dehydrogenase BetB from *Staphylococcus aureus*: structure-based mutational studies

Chao Chen, Jeong Chan Joo, Greg Brown, Ekaterina Stolnikova, Andrei Halavaty, Alexei Savchenko, Wayne F. Anderson, Alexander F. Yakunin

Supplementary Table S1. Apparent kinetic parameters of the wild-type and mutant BetB proteins.

Proteins	The location of residues	K_m (mM)	K_i (mM)	k_{cat} (s^{-1})	k_{cat}/K_m (s^{-1} mM^{-1})	K_m (NAD^+, mM)
BetB-WT[a]		0.17 ± 0.03	0.34 ± 0.06	11.0 ± 1.4	64.7	0.43 ± 0.03
A107N[b]	BA	0.41 ± 0.02	0.48 ± 0.03	11.9 ± 1.0	29.0	1.28 ± 0.09
D111A[b]	BA	0.24 ± 0.02	2.76 ± 0.31	0.40 ± 0.04	1.67	0.80 ± 0.06
T154A[a]	Adenine	0.26 ± 0.02	0.41 ± 0.10	8.57 ± 0.66	33.0	0.65 ± 0.05
L161M[c]	Nicotinamide & BA	2.69 ± 0.45	0.96 ± 0.25	10.2 ± 2.5	3.79	0.11 ± 0.01
L210F[a]	Ribose	0.94 ± 0.07	0.10 ± 0.01	14.2 ± 1.4	15.1	0.87±0.09
S214K[a]	Adenine	0.44 ± 0.26	0.24 ± 0.15	12.0 ± 5.56	27.3	1.01 ± 0.07
M220L[a]	Adenine	0.38 ± 0.14	0.37 ± 0.14	11.5 ± 2.2	30.3	0.71 ± 0.03
S221T[a]	Adenine	0.10 ± 0.02	0.48 ± 0.10	4.78 ± 0.59	47.8	0.29 ± 0.01
F231L[c]	Adenine	0.44 ± 0.05	2.96 ± 0.16	1.60 ± 0.14	3.64	0.25 ± 0.01
E236A[a]	pyrophosphate	0.14 ± 0.02	0.48 ± 0.08	7.40 ± 0.76	52.9	0.88 ± 0.07
N244H[b]	Adenine	0.56 ± 0.08	0.56 ± 0.06	6.50 ± 0.76	11.6	1.81 ± 0.24
F283Y[a]	BA	0.35 ± 0.01	0.24 ± 0.03	13.3 ± 1.1	38.0	1.01 ± 0.06
I332S[b]	pyrophosphate	0.66 ± 0.10	0.74 ± 0.13	1.18 ± 0.14	1.79	0.79 ± 0.03
E335A[a]	pyrophosphate	0.19 ± 0.02	0.43 ± 0.05	11.9 ± 1.1	62.6	0.85 ± 0.08
K339R[a]	pyrophosphate	0.39 ± 0.02	0.38 ± 0.03	12.2 ± 0.9	31.3	0.63 ± 0.06
Y343A[c]	pyrophosphate	0.77 ± 0.16	1.98 ± 0.12	0.21 ± 0.03	0.27	0.44 ± 0.03
P449M[b]	BA	0.33 ± 0.05	1.99 ± 0.15	7.37 ± 0.67	22.3	0.39 ± 0.03
M220L/S221T[a]	Adenine	0.28 ± 0.11	0.28 ± 0.11	10.5 ± 1.6	37.5	0.60 ± 0.01

All reactions were performed at pH 8.0 and 30°C, using varied BA at 5 mM NAD^+, or varied NAD^+ at different concentrations of BA: [a]0.2-0.3 mM, [b]0.5-0.8 mM, [c]1-5 mM.

Supplementary Figure Legends

Supplementary Figure S1. Substrate profile of the *S. aureus* BetB dehydrogenase (dehydrogenase activity against different substrates). The dehydrogenase activity was determined using 1 mM substrate, 1 mM NAD^+ and 10 μg of BetB.

Supplementary Figure S2. Inhibition patterns of the *S. aureus* BetB dehydrogenase activity by NADH (A, B) and GB (C, D). A, Dehydrogenase activity of BetB as a function of NAD^+ concentration in the presence of various concentrations of NADH: 2.5 μM (closed circles), 25 μM (open circles), 50 μM (closed triangles) and 100 μM (open triangles). BA concentration was 0.15 mM. The control (0 μM NADH) has the same line as 2.5 μM NADH. **B**, Dehydrogenase activity of BetB as a function of BA concentration in the presence of various concentrations of NADH: 100 μM (closed circles), 250 μM (open circles), 375 μM (closed triangles) and 500 μM (open triangles). The control (0 μM NADH) has the same line as 100 μM NADH. **C**, Dehydrogenase activity of BetB as a function of NAD^+ concentration in the presence of various concentrations of GB (mM): 0 (closed circles), 10 (closed triangles up), 50 (closed triangles down) and 200 (closed square). BA concentration was 0.15 mM. **D**, Dehydrogenase activity of BetB as a function of BA concentration in the presence of various concentrations of GB (mM): 0 (closed circles), 10 (closed triangles up), 50 (closed triangles down) and 200 (closed square).

Supplementary Figure S3. Inhibition patterns of the BetB inhibition by dead-end inhibitors. (**A**, **B**), Dehydrogenase activity of BetB as a function of NAD^+ concentration (**A**) or BA concentration (**B**) in the presence of various concentrations of choline: 0 mM (closed circles), 1 mM (open circles), 10 mM (closed triangles), 50 mM (open triangles) and 200 mM (squares). (**C**, **D**), Dehydrogenase activity of BetB as a function of NAD^+ concentration (**C**) or BA concentration (**D**) in the presence of various concentrations of benzaldehyde: 0 mM (closed circles), 0.1 mM (open circles), 0.5 mM (closed triangles) and 2 mM (open triangles).

Supplementary Figure S4. Structure-based sequence alignment of BetB and other BADHs. The amino acid sequences of four BADHs were aligned using Clustal Omega (http://www.ebi.ac.uk/Tools/msa/clustalo/). The secondary structure elements of BetB (PDB codes 4MPY) and YdcW (PDB code 1WNB) are shown above and below the alignment, respectively. The secondary structure elements are shown; α (an α-helix), β (a β-strand), TT (a β-turn) and η (a 3_{10} helix). The conserved residues are shown in red background including the BetB nucleophile Cys289 and the catalytic base Glu255. The residues mutated in this study are indicated by closed triangles. The proteins compared are BetB from *S. aureus* (SA2613; UniProtKB ID Q9L4P8), SoBADH from *S. oleracea* (UniProtKB ID P17202), PaBADH from *P. aeruginosa* (UniProtKB ID Q9HTJ1), and YdcW from *E. coli* (UniProtKB ID P77674).

Supplementary Figure S5. Structural basis of BetB inhibition by BA: productive and non-productive binding of BA. Docking simulation of BA binding in the active

sites of the wild-type BetB (**A, B**) and the homology model of Q162M (**C, D**), V288D (**E**), and S290T (**F**). Panels A, C, E and F represent the productive binding mode of BA, with a hydrogen bond formed between carbonyl group of BA and the backbone nitrogen atom of Cys289. In contrast, panel B and D present BA in a non-productive binding mode with the similar binding affinity, and a hydrogen bond formed between carbonyl group of BA and amide group of Asn157. The amino acid side chains and ligands are shown as sticks and labeled.

Supplementary Figure S6. The cofactor binding site of the wild-type BetB (A) and G234S (B). The amino acid side chains and NAD are shown as sticks and labelled along with the protein ribbon.

Supplementary Figure S1.

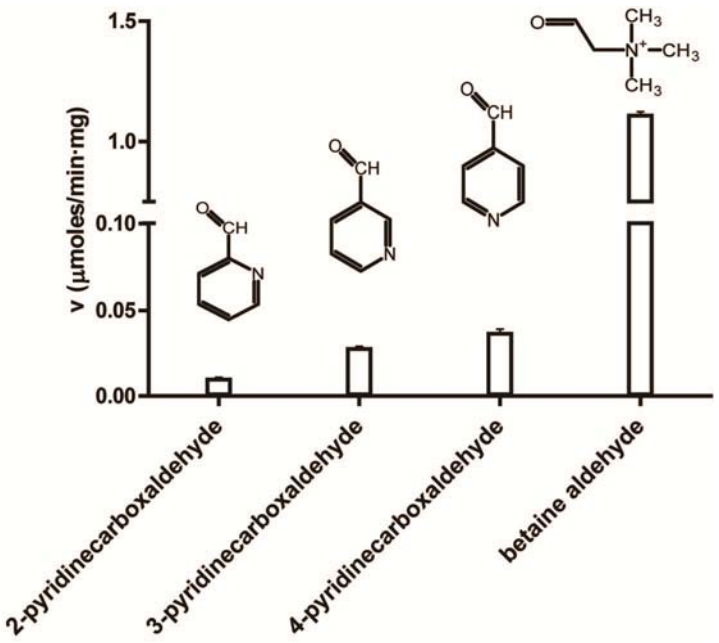

Supplementary Figure S2.

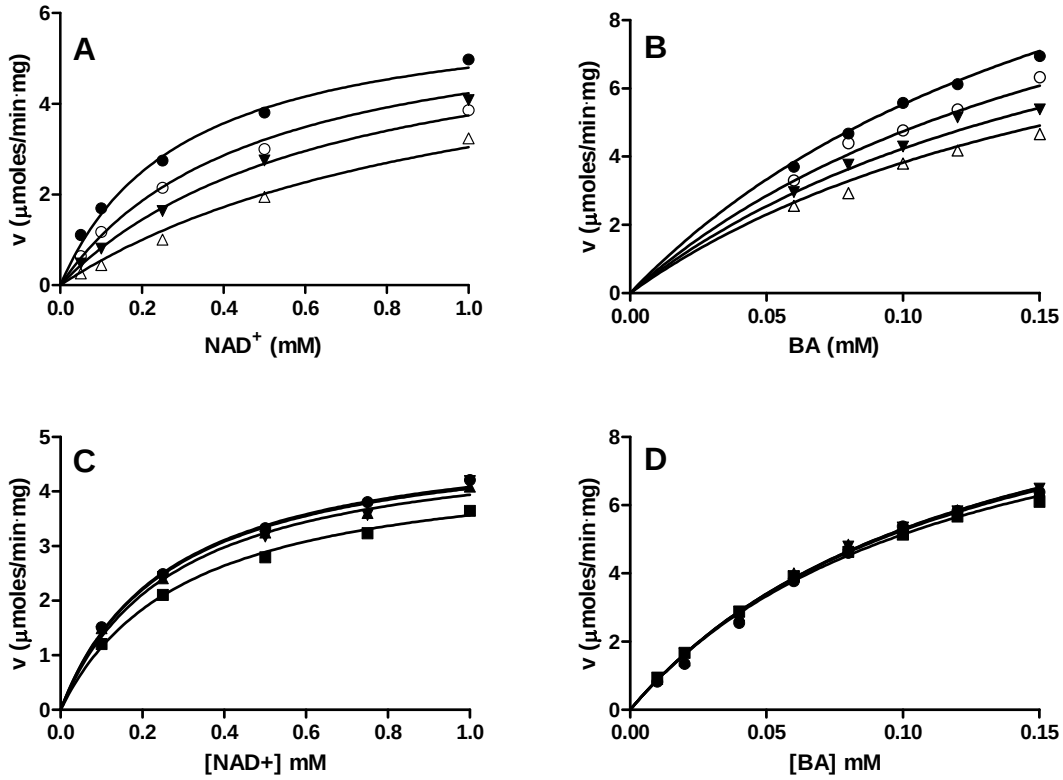

Supplementary Figure S3.

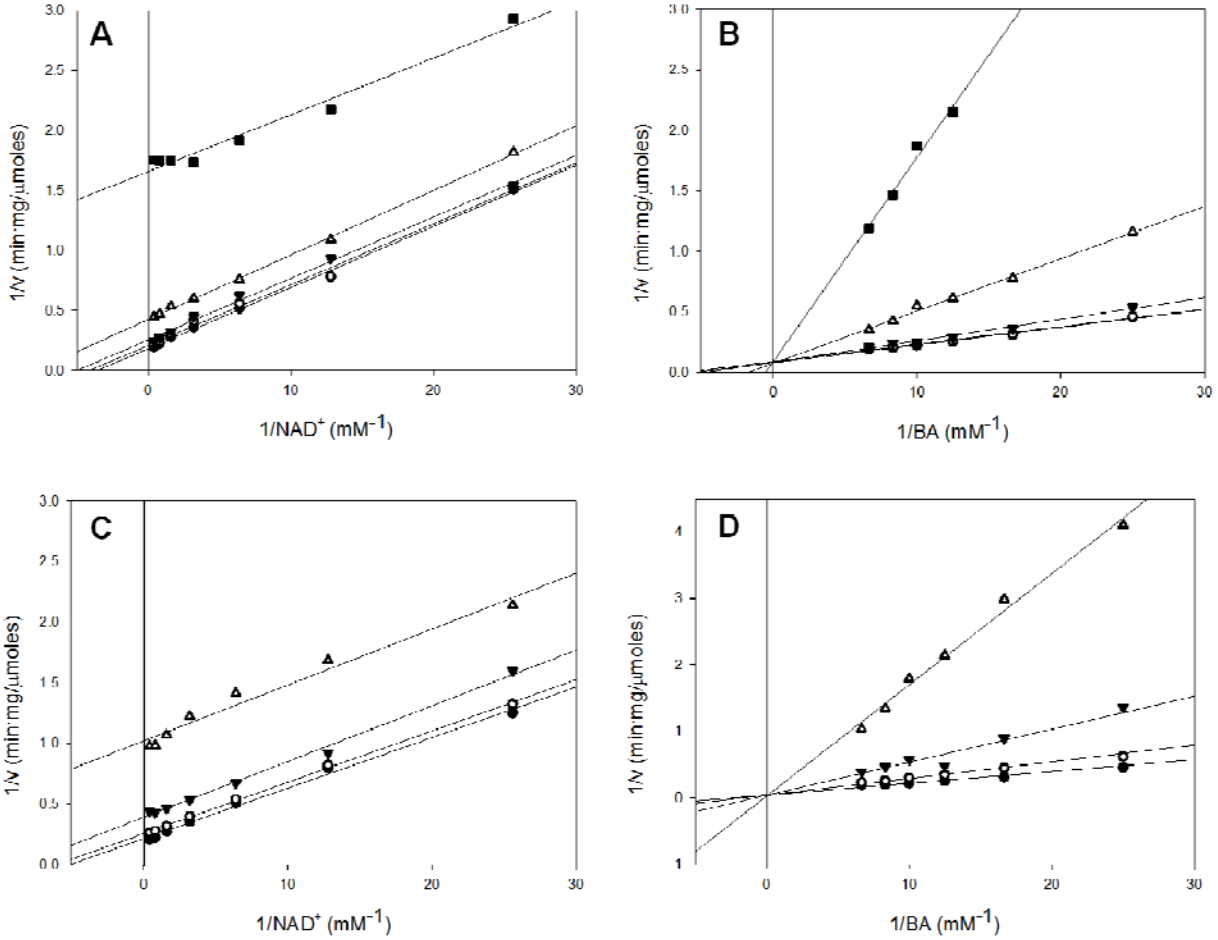

Supplementary Figure S4.

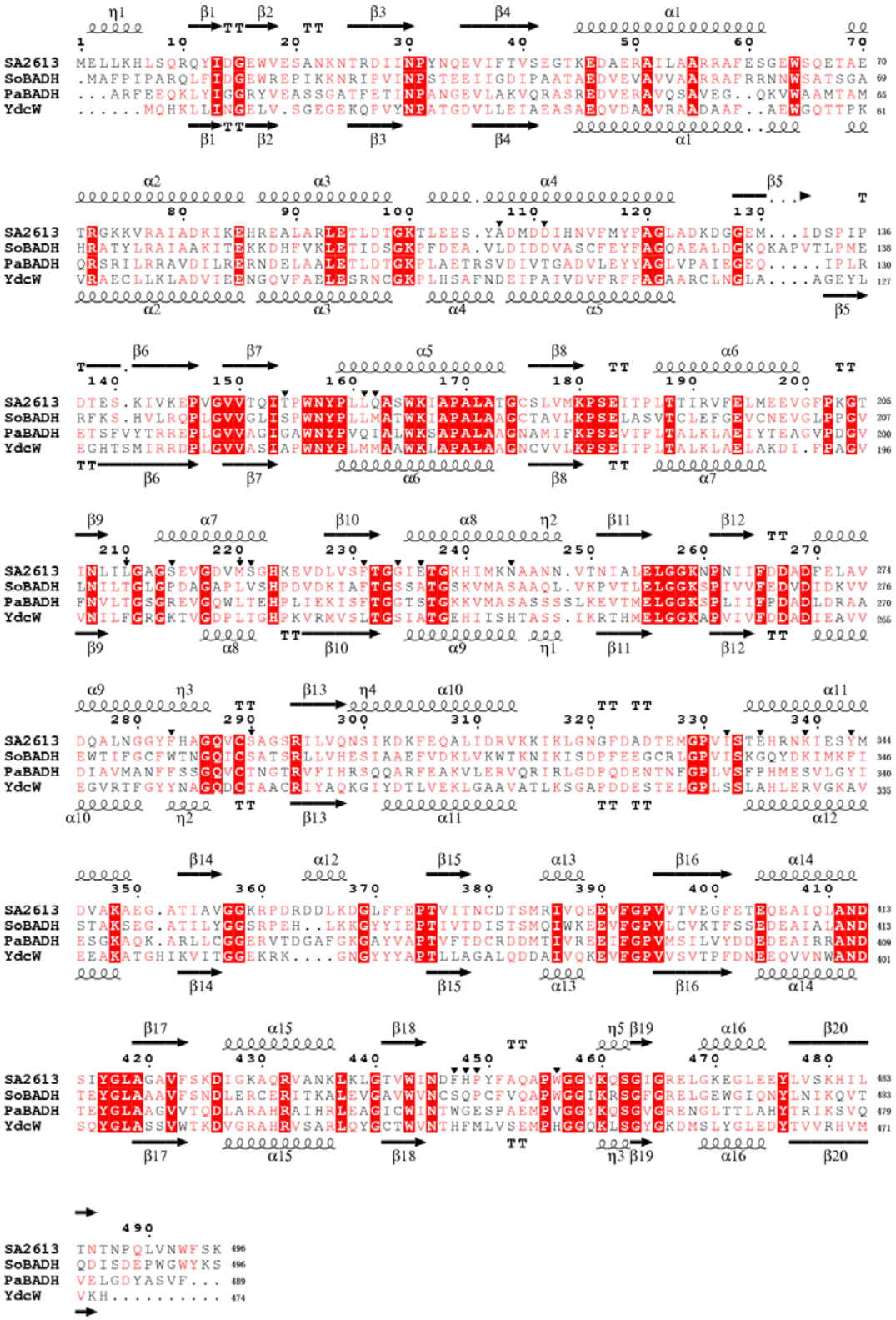

Supplementary Figure S5.

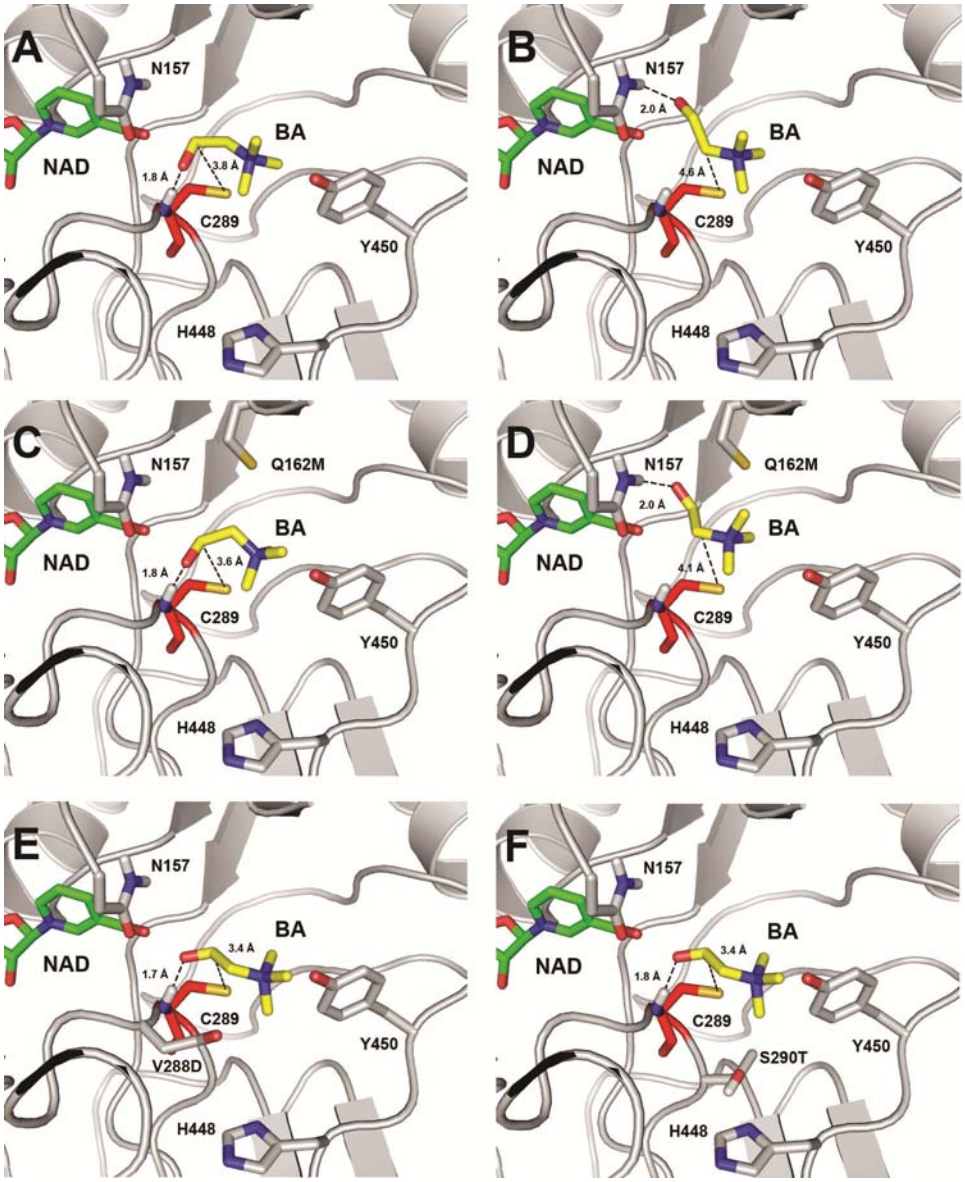

Supplementary Figure S6.